

## Long-term changes on estuarine ciliates linked with modifications on wind patterns and water turbidity

López-Abbate M. Celeste <sup>1,\*</sup>, Molinero Juan-Carlos <sup>2</sup>, Perillo Gerardo M.E. <sup>1</sup>, Barría De Cao M. Sonia <sup>1</sup>, Pettigrosso Rosa E. <sup>3</sup>, Guinder Valeria A. <sup>1</sup>, Uibrig Roman <sup>1</sup>, Berasategui Anabela A. <sup>1</sup>, Vitale Alejandro <sup>1</sup>, Marcovecchio Jorge E. <sup>1,4,5</sup>, Hoffmeyer Mónica S. <sup>1</sup>

<sup>1</sup> Instituto Argentino de Oceanografía (CONICET-UNS), Camino La Carrindanga Km 7.5, 8000, Bahía Blanca, Argentina

<sup>2</sup> Institut de Recherche pour le Développement (IRD), UMR248 MARBEC, IRD/CNRS/IFREMER/UM, Sète Cedex, France

<sup>3</sup> Departamento de Biología, Universidad Nacional del Sur, Av. Alem 1253, 8000, Bahía Blanca, Argentina

<sup>4</sup> Universidad Tecnológica Nacional, Facultad Regional Bahía Blanca (UTN-BHI), 11 de Abril 461, 8000, Bahía Blanca, Argentina

<sup>5</sup> Universidad FASTA, Facultad de Ingeniería, Gascón 3145, 7600, Mar del Plata, Argentina

\* Corresponding author : Celeste M. López-Abbate, email address : [mclabbate@iado-conicet.gob.ar](mailto:mclabbate@iado-conicet.gob.ar)

### Abstract :

Planktonic ciliates constitute a fundamental component among microzooplankton and play a prominent role in carbon transport at the base of marine food webs. How these organisms respond to shifting environmental regimes is unclear and constitutes a current challenge under global ocean changes. Here we examine a multiannual field survey covering 25 years in the Bahía Blanca Estuary (Argentina), a shallow, flood-plain system dominated by wind and tidal energy. We found that the estuary experienced marked changes in wind dominant regimes and an increase in water turbidity driven from the joint effect of persistent long-fetch winds and the indirect effect of the Southern Annular Mode. Along with these changes, we found that zooplankton components, i.e. ciliates and the dominant estuarine copepod *Acartia tonsa*, showed a negative trend during the period 1986–2011. We showed that the combined effects of wind and turbidity with other environmental variables (chlorophyll, salinity and nutrients) consistently explained the variability of observed shifts. Tintinnids were more vulnerable to wind patterns and turbidity while showed a loss of synchrony with primary productivity. Water turbidity produced a dome-like pattern on tintinnids, oligotrichs and *A. tonsa*, implying that the highest abundance of organisms occurred under moderate values (~50 NTU) of turbidity. In contrast, the response to wind patterns was not generalizable probably owing to species-specific traits. Observed trends denote that wind-induced processes in shallow ecosystems with internal sources of suspended sediments, are essential on ciliate dynamics and that such effects can propagate through the interannual variability of copepods.

---

## Highlights

► Planktonic ciliate's abundance decreased over the last 25 years in a shallow estuary. ► Decreasing cell abundance was linked to changes in wind dominant regimes and increased water turbidity. ► Tintinnids were more vulnerable to wind patterns and turbidity and lost synchrony with primary productivity. ► Interannual variability of the copepod *Acartia tonsa* followed the changes in ciliate community. ► Erosive processes in shallow estuaries impact on the interannual dynamics of ciliates and such effects can cascade-up to copepods.

**Keywords** : Tintinnids, Oligotrichs, *Acartia tonsa*, Wind, Turbidity, Estuaries

## 42 **Introduction**

43 In coastal ecosystems, tintinnids and oligotrichs (hereafter collectively referred to as  
44 'ciliates'), constitute a fundamental component among microzooplankton and play a  
45 prominent role in carbon transport at the base of marine food webs (Keller and Hood 2011,  
46 Mitra et al. 2014, Legendre and Rivkin 2015). They rapidly synchronize productivity  
47 patterns due to their short generation time and graze an average of 60 % of daily primary  
48 production and 10 % of daily bacterial production (Steinberg and Landry 2017), while  
49 representing nearly 30 % of copepods diet (Calbet and Saiz 2005). In spite of their  
50 relevance in both trophic dynamics and carbon fluxes, ciliate's responses to environmental  
51 drivers remain elusive due to the lack of sustained long-term surveys and synoptic  
52 approaches (Clamp and Lynn 2017). Empirical evidence has shown a prominent role of  
53 temperature and food on ciliate's dynamics, however, the long-term response of these  
54 organisms is shaped by a variety of additional drivers (Dolan and Gallegos 2001, Aberle et  
55 al. 2013, López-Abbate et al. 2015). Hence, we urgently need sustained field observations  
56 that integrate ecological responses of natural communities to multi-scale drivers (Heger et  
57 al. 2014). Sustained observations of wide-varying environments are critical to understand  
58 underlying mechanisms shaping the structure and function of plankton communities (Boyd  
59 and Hutchins 2012) and to detect non-linearities (Kreyling et al. 2018). This information  
60 will ultimately facilitate the anticipation of inefficient carbon transfer toward higher trophic  
61 levels (Wohlers et al. 2009).

62 Among shallow estuaries, surface winds have an important influence on the seasonal  
63 pattern of plankton (Reynolds 2006). This influence is driven by physical processes such as  
64 waves, currents, microscale turbulence and particles resuspension (Scully et al. 2005, Li  
65 and Li 2011, Whipple et al. 2018). Microscale turbulence induced by surface winds, for

66 instance, reduces the sinking velocity of suspended organisms and can enhance prey  
67 capture and nutrient uptake (Kiørboe and Saiz 1995, Barton et al. 2014, Pécseli et al. 2014).  
68 In addition, the transport of inorganic nutrients toward illuminated layers produced by  
69 wind-driven water mixing, regulates phytoplankton growth and availability (Kiørboe 2008).  
70 In flood-plain estuaries, wind-induced currents and wind waves are among the most  
71 important factors that favour sediment resuspension in the water column, and profoundly  
72 interfere with the light penetration (Weir and McManus 1987, Brand et al. 2010, Bever et  
73 al. 2018). A high concentration of suspended particles, in turn, can restrict ciliate  
74 reproduction (Jack and Gilbert 1993), while handling-limited predation by the interference  
75 of inedible suspensoids with prey uptake has been observed in planktonic filter feeders such  
76 as cladocerans (Laspoumaderes et al. 2017).

77 Located in the SW Atlantic Ocean, the Bahía Blanca Estuary is a shallow, flood-plain  
78 estuary dominated by wind and tidal energy (Piccolo and Perillo 1990). In the last decades,  
79 the region has experienced climate-driven environmental changes encompassing warmer  
80 winters and extreme dry periods (Aravena and Luckman 2009, Guinder et al. 2010), along  
81 with persistent positive anomalies of the Southern Annular Mode (SAM). Such anomalies  
82 are associated with stronger than normal westerlies over the mid-high-latitudes and weaker  
83 westerlies in the mid-latitudes (Marshall 2003). Concurrently, water turbidity has shown a  
84 positive trend in the last 15 years, presumably as a response to wind shifts and the lateral  
85 erosion of salt marshes associated with sea level rise (Pratolongo et al. 2013, López-Abbate  
86 et al. 2017). Modelling approaches revealed the emergence of both, wind speed and water  
87 turbidity, as dominant factors driving the decline of chlorophyll concentration in recent  
88 years (López-Abbate et al. 2017), however, the interannual response of phagotrophic  
89 plankton has been so far overlooked. Ciliates contribute with the highest carbon biomass

90 within estuarine microzooplankton during the entire annual cycle. Experimental approaches  
91 have revealed that these organisms are the preferred food source of the dominant copepod  
92 *Acartia tonsa* (Diodato and Hoffmeyer 2008). This omnivorous species cohabits with  
93 ciliates during most of the year whereas it may reach up to 90 % of total mesozooplankton  
94 abundance during the warm season, concurrent with the highest annual concentration of  
95 tintinnids (Hoffmeyer 2004). In turn, *A. tonsa* is one of the main food sources of  
96 planktivorous fish (López Cazorla et al. 2011). The aim of this study is to quantify the  
97 interannual response of ciliates to environment drivers, with emphasis on wind patterns and  
98 water turbidity. For this purpose, we have employed a unique multiannual data set in the  
99 SW Atlantic Ocean that covered the abundance of micro- (ciliates community) and meso-  
100 zooplankton (*A. tonsa*) along with an exhaustive environmental data set. To quantify the  
101 effect of multiple drivers on ciliates and *A. tonsa*, we used Boosted Regression Trees  
102 (BRT). The analyses are organized in the following steps: 1) exploration of top-down and  
103 bottom-up interactions, 2) testing of the hypothetical cause-effect models, 3) identification  
104 of dominant drivers according to the amount of explained deviance and 4) comparison of  
105 the partial response of zooplankton groups to wind patterns and water turbidity.

106

## 107 **Materials and Methods**

### 108 *Study area*

109 The Bahía Blanca Estuary (38°42'-39°25'S, 61°50'-62°22'W) is located in a temperate,  
110 semiarid region at the northern boundary of Patagonia in the SW Atlantic coast, Argentina.  
111 Mesotidal setting and wind-driven mixing prevents stratification during most of the year  
112 (Perillo et al. 2001). The depth of the estuary ranges between 1 and 24 m, while the mean

113 value is about 10 m (Perillo et al. 2001). Half of the estuarine basin consists of extensive  
114 low-slope tidal flats densely fragmented by tidal courses (Perillo 2009) oriented NW–SE  
115 (Fig. 1). The feature promotes an intense interaction between the water column and the  
116 bottom layers, whose first 3-4 m are composed by a massive deposit of unstructured mud  
117 (Pratolongo et al. 2017). Predominant NW winds run parallel to the estuarine main  
118 channels and produce high energy wind waves that enhances the erosion of tidal flats  
119 (Perillo and Sequeira 1989, Pratolongo et al. 2010). Grain size in the lower mudflats are in  
120 the very coarse to fine silt range (mode of 32  $\mu\text{m}$ ), while suspended sediments size in the  
121 water column varies between 1 and 50  $\mu\text{m}$  (mode of 10  $\mu\text{m}$ ) (Guinder et al. 2015, Zapperi  
122 et al. 2017).

123 The main estuarine channel is periodically dredged since 1958, while the harbour basin in  
124 the inner reach is water-jettied to prevent sediment deposition. The dredged volume  
125 increased 11-fold after 1999 due to the deepening and widening of the access channel.  
126 Currently, dredging operations are executed along an area of 20 km long and 190 m width  
127 and attain a regular depth of 13.5 m (López-Abbate et al. 2017). As a result, the volume of  
128 sediment extraction by dredging significantly increased from a yearly mean of 240,714  $\text{m}^3$   
129 in 1958-1998, to 2,657,919  $\text{m}^3$  in 1999-2011. In addition, the development of urban centres  
130 fostered point-source nutrient loading, which can sporadically exceed the tolerance of  
131 microzooplankton due to the toxic effect of ammonium (López-Abbate et al. 2015).

132

### 133 *Biological data*

134 Microzooplankton samples were taken from the surface layer using a van Dorn Bottle (2.5  
135 l) in the inner zone of the estuary (Puerto Cuatros, 38°-50'S, 62°20'W) (Fig. 1), at a  
136 monthly frequency during discontinuous periods from 1986 to 2011. The quantification of

137 ciliates was done by settling a variable volume (10-50 ml, depending on sediment and  
138 plankton concentration) of preserved seawater sample (neutral Lugol's iodine, f.c. 10 %) in  
139 Utermöhl chambers during 24 h. The entire chamber was analysed under a Wild M20  
140 inverted microscope (Hasle 1978). We here focused on tintinnids and oligotrichs since they  
141 represent the most abundant groups within microzooplankton in the Bahía Blanca Estuary  
142 (Pettigrosso 2003, Barría de Cao et al. 2005). A total of 178 samples were analysed for the  
143 quantification of tintinnids, while 97 samples were analysed for the quantification of  
144 oligotrichs. Samples for tintinnids quantification were taken at a monthly or biweekly  
145 frequency during the following periods: April 1986 to May 1989, June 1995 to April 1997,  
146 March 2002 to March 2004, October 2006 to February 2008 and July 2008 to April 2011.  
147 Samples for oligotrichs quantification were also taken at a monthly or biweekly frequency  
148 during the following periods: February 1994 to February 1995, January 2007 to February  
149 2008, July 2008 to April 2011. Tintinnids were identified to the species level, while  
150 oligotrichs were in some cases identified to the genus level while in other cases they were  
151 counted as a whole. From 1978 to 2009, samples for chlorophyll *a* analysis were taken  
152 uninterruptedly at the same location, on a fortnightly basis. Chlorophyll *a* concentration  
153 was quantified by the extraction with acetone (90 %) at a controlled room temperature and  
154 then refrigerated in the dark at 4 °C for 24 h. Then the samples were centrifuged and the  
155 supernatant separated. The pigment concentration was determined by spectrophotometry  
156 (Jenway 6715 UV-Vis) using the equations of Lorenzen (1967). To assess predator-prey  
157 links we also included data on the dominant copepod species, *A. tonsa*, which is a key  
158 component of the estuarine food web. Adults of *A. tonsa* were obtained from  
159 mesozooplankton samples collected at a monthly frequency during the following periods:  
160 July 1979 to August 1980, August 1982 to September 1983, July 1990 to August 1991,

161 April 2002 to November 2002, January 2007 to February 2008, July 2008 to December  
162 2010 and January 2015 to December 2015. Samples were collected with subsurface  
163 horizontal tows using a 200  $\mu\text{m}$  mesh plankton net and 0.30 m mouth diameter equipped  
164 with a Hydrobios flowmeter and towed for 10 min at a constant speed of 2 knots. Surface  
165 sampling bias was minimized by reproducing the sampling protocol and the subsequent  
166 sample treatment throughout the studied period. Samples were fixed (4 % formalin) and  
167 analysed under a Wild M5 stereoscopic microscope using a Bogorov chamber following the  
168 methodology proposed by Boltovskoy (1981).

169

#### 170 *Environmental data*

171 Water temperature ( $^{\circ}\text{C}$ ), salinity and turbidity (NTU) were measured simultaneous to  
172 biological sampling using a digital multi-sensor Horiba U-10. Likewise, samples for the  
173 determination of dissolved inorganic nutrients were taken from the surface layer using a  
174 van Dorn Bottle (2.5 l) at a monthly frequency. Nitrate, nitrite, phosphate and silicate  
175 concentrations were determined following the methods described in Spetter et al. (2015).  
176 The sum of nitrate and nitrite was expressed as the concentration of dissolved inorganic  
177 nitrogen (DIN). Data on wind speed and direction were provided by the National Weather  
178 Service (<http://www.smn.gov.ar>). Hourly data were available for the period 1991-2015  
179 while previous to 1991 (1978-1990) data were recorded every three hours.

180 The region is influenced by large-scale atmospheric phenomena such as SAM and El Niño  
181 Southern Oscillation (ENSO) (Vera et al. 2004, Menéndez and Carril 2010). The SAM-  
182 Marshall index, based on the difference of mean sea level pressure between the latitudes  
183  $40^{\circ}\text{S}$  and  $65^{\circ}\text{S}$ , was selected for the analysis as it reduces the influence of spurious trends  
184 of reanalysis products (Marshall 2003). The temporal evolution of ENSO was assessed by

185 the SST averaged anomaly in the Niño 3.4 region (Niño 3.4 index) in the central-east  
186 region of the Tropical Pacific Ocean (5°N–5°S, 170°–120°W) (Trenberth 1997). The  
187 atmospheric variables used to assess indirect effect of climate modes on wind patterns were  
188 air temperature and sea level pressure. Monthly record covered the northern SW Atlantic  
189 coast including the estuarine area and extending from -35.0 to -42.5 °N and from 295.0 to  
190 302.5 °E. Regional atmospheric variables as well as the standardized modes of atmospheric  
191 variability were obtained from the Climate Diagnostics Center (NCEP/NCAR) reanalysis  
192 fields.

193

#### 194 *Data analysis*

##### 195 *Identification of trends in biological data*

196 Owing to the different frequency and time-coverage of time series, all records were  
197 screened and averaged to obtain monthly values prior the analysis. To evaluate the  
198 influence of co-occurring environmental drivers on the interannual response of ciliates and  
199 the copepod *A. tonsa*, we first analysed the general trend of tintinnids and oligotrichs  
200 abundance by fitting a linear model on monthly records as a function of time. The long-  
201 term variability of log-transformed abundance of the three zooplankton groups and wind  
202 speed were also fitted to linear models to compute the yearly rate of change. In addition, the  
203 long-term trend of individual tintinnid's species was displayed in a heat map using the  
204 annual mean of log-transformed abundance. The phenology of tintinnids, whose sampling  
205 frequency allowed a more detailed examination, was evaluated using Generalized Additive  
206 Model (GAM). For this purpose, we compared the annual cycle using mean monthly  
207 records as a function of time (months) during two periods: 1986-2002 and 2003-2011.  
208 These periods were selected considering the significant breakpoint on the chlorophyll *a*

209 time series noticed in 2002 (López-Abbate et al. 2017) and assuming a bottom-up linkage  
210 between tintinnids and chlorophyll.

211

212 *Interconnection between climate modes, regional atmospheric variability and water*  
213 *turbidity*

214 Wind patterns along the period 1991-2015 were visualized through annual wind roses with  
215 the R-function `plot.windrose` (R Development Core Team 2014). Hourly data were  
216 employed to plot the frequency of wind speed and direction by year. Records previous to  
217 1991 were not plotted due to lower than hourly data frequency. The percentage of ‘calms’,  
218 defined as the fraction of zero wind speed along the year, was calculated by the `windRose`  
219 function from the R-package `openair`. To improve the visualization of long-term trends,  
220 annual means of wind speed, wind direction and water turbidity were fitted as a function of  
221 time by a GAM. Yearly records in the period 1978-2015 were fitted with a logit link  
222 function using the R-package `mgcv`.

223 To explore correlations between water turbidity and wind patterns with climate variables of  
224 interest operating at regional and global scales, we constructed a path model (SEM). We  
225 first constructed the theoretical model by ranking the explanatory variables, from global  
226 (ENSO, SAM), regional (air temperature and sea level pressure) and local scale variables  
227 (precipitation, wind speed, wind direction and SST), to the response variable (water  
228 turbidity), thus assuming causal relationships. ENSO and SAM signals are known to co-  
229 vary during austral summer (Fogt et al. 2011), therefore they were set as covariates in the  
230 model. Path coefficients were determined by simple and partial multivariate regression and  
231 Monte Carlo permutation tests (1000 replicates), while the Chi-square values were used to

232 assess the robustness of models (Alsterberg et al. 2013). Path analysis was performed using  
233 the R-package lavaan.

234

### 235 *Influence of environmental drivers on plankton groups*

236 Once defined the long-term modifications on ciliate community, we identified the  
237 environmental variables driving such changes by means of Regression Tree Models.  
238 Regression Trees are non-linear predictive models that can be used when data have lots of  
239 features which interact in nonlinear ways. The method is based on the partition of the  
240 predictor space into rectangles until data fragments can fit simple models. Predictors and  
241 split points are chosen to minimize prediction errors, which is calculated as the sum of  
242 squared errors between the predicted values and the actual values (Breiman et al. 1984,  
243 De'ath and Fabricius 2000). We here used Boosted Regression Tree (BRT) which combines  
244 simple models (trees) to gain predictive power (Elith et al. 2008). The number of times a  
245 predictor is selected for splitting and the amount of explained deviance, allow to rank  
246 predictive variables according to their relative importance. The R-packages gbm and dismo  
247 were employed for the construction of BRT. Models were trained by setting the log-  
248 transformed abundance of tintinnids and oligotrichs as the response variables, and  
249 chlorophyll *a* concentration, wind speed, wind direction, salinity, turbidity and dissolved  
250 inorganic nutrient concentration (DIN, phosphate and silicate) as the explanatory variables.  
251 Given the positive correlation between ciliates and chlorophyll *a* concentration with the  
252 abundance of *A. tonsa* (Diodato and Hoffmeyer 2008), we assumed that the ecological  
253 interaction among groups was dominated by the bottom-up control exerted upon the  
254 copepod. Thus we constructed an additional model using the abundance of *A. tonsa* as the  
255 response variable and the concentration of ciliates and chlorophyll *a*, wind speed, wind

256 direction, salinity and turbidity as the explanatory variables. The lack of data regarding the  
257 loss of *A. tonsa* by fish predation, as well as other unobservable factors, can significantly  
258 reduce the predictive power of models. In BRT, pre-selection of variable is not required  
259 since the model largely ignores non-informative predictors when fitting trees (Elith et al.  
260 2008). Sea surface temperature (SST), nevertheless, was not included to avoid spurious up-  
261 weighting due to autocorrelation. The marked seasonality of ciliates and *A. tonsa*, may  
262 further contribute to the up-weighting of SST in BRT models. Model fitting was evaluated  
263 by the cross-validation deviance and standard error. Given that wind speed, wind direction  
264 and turbidity explained more than 29% of variance when predicting the abundance of  
265 zooplankton groups, we examined the partial response of tintinnids, oligotrichs and *A.*  
266 *tonsa* to these three predictors.

267

## 268 **Results**

### 269 *Long-term dynamics of ciliates*

270 The mean monthly abundance of tintinnids along the time series was 3416 cell l<sup>-1</sup> (Table  
271 S1), while the monthly abundance of oligotrichs was lower and averaged 1403 cell l<sup>-1</sup>  
272 (Table S2). The assessment of the long-term variation of ciliates showed a negative  
273 interannual trend (Fig. 2). Tintinnids declined at a yearly rate of 2.8 % (p<0.001, R<sup>2</sup>=  
274 0.735), corresponding to a decrease of ~97.8 cell l<sup>-1</sup> yr<sup>-1</sup>, while oligotrichs declined at a  
275 yearly rate of 1.6 %, although the trend was not significant (p=0.221, R<sup>2</sup>=0.281). Likewise,  
276 the abundance of the copepod *A. tonsa* also showed a negative trend (p=0.005, R<sup>2</sup>=0.605)  
277 and a yearly rate of decline of 3.3 %. A total of 11 tintinnid species showed a negative  
278 trend, including the dominant species *Tintinnidium balechi*, while *Tintinnopsis brasiliensis*  
279 and *T. sp.* showed a positive trend, and *Metacylis aff. mereschkowskyi*, *T. buetschlii*, *T.*

280 *buetschlii* var. *mortensenii*, *Favella taraikaensis* *Leprotintinnus pellucidus* and *T. amphora*  
281 showed only occasional occurrence (Table S1, Fig. 3). The most abundant species within  
282 ciliates throughout the time series was *T. balechi*, which represented an average of 27 % of  
283 total abundance and revealed a steeper rate of decline (4.3 %,  $p=0.008$ ,  $R^2=0.425$ , data not  
284 shown) compared with total tintinnid abundance. The percentage decline represented a  
285 decrease of 52.4 ind  $l^{-1} yr^{-1}$ . The annual cycle of tintinnids before and after 2003 revealed  
286 the loss of the spring pulse that followed the winter phytoplankton bloom in recent years  
287 (Fig. 4).

288

#### 289 *Trends in environmental conditions*

290 Wind speed showed a slowdown rate of  $0.4 m s^{-1} y^{-1}$  since 1998 to date (linear regression  
291 model:  $p<0.001$ ,  $R^2=0.680$ ), which represents a decline of 32.7 % (Fig. 5, Fig. 6a). During  
292 the period 1986-2002, wind speed averaged  $6.51 m s^{-1}$  while the mean annual wind speed in  
293 the following period (2003-2015) was  $5.71 m s^{-1}$ . Mean annual wind direction showed  
294 higher persistence toward of NW quadrant since the 1978 to date (linear regression model:  
295  $p<0.001$ ,  $R^2=0.480$ ) (Fig. 5, Fig. 6a). In addition, the percentage of calm periods declined at  
296 a yearly rate of 2 % since the beginning of the time series (linear regression model:  
297  $p<0.001$ ,  $R^2=0.509$ ). Water turbidity increased accordingly after 1999 (Fig. 6a) at a yearly  
298 rate of 4 % ( $p<0.001$ ,  $R^2=0.745$ ), while SEM revealed that in the period 1978-2011, it  
299 responded to the direct effect of wind speed, wind direction and SST and to the indirect  
300 effect of SAM and ENSO ( $X^2=450.49$ ,  $df=12$ ,  $p<0.001$ , Fig. 6b). Mean annual SST and  
301 salinity was  $15.7 ^\circ C$  and 33.2 respectively, and both variables evidenced no linear trends  
302 along the time series. Positive trends were observed in the mean annual concentration of  
303 DIN ( $p=0.002$ ,  $R^2=0.290$ ) and phosphate ( $p<0.001$ ,  $R^2=0.470$ ), while no evident trend was

304 observed in the concentration of silicate. Mean annual concentration of DIN, phosphate and  
305 silicate was 6.90, 2.07 and 90.37  $\mu\text{M}$  respectively, while the yearly rate of DIN and  
306 phosphate increase was 1.1 and 0.8 % respectively.

307

308 *Environmental drivers of ciliates and A. tonsa abundance*

309 BRT yielded evidence of the response of tintinnids ( $R^2=0.528$ ), oligotrichs ( $R^2=0.982$ ) and  
310 *A. tonsa* ( $R^2=0.435$ ) to environmental variables. The ranking of driver importance (Fig. 7)  
311 revealed that the optimal predictors of tintinnid abundance were turbidity, wind speed, wind  
312 direction and DIN, which explained 25.9, 22.3, 14.0 and 13.1 % of total tintinnids  
313 variability, respectively. Predictors that better explained the variability of oligotrichs were  
314 phosphate (34 %), silicate (26.5 %), wind speed (25.1 %) and turbidity (12.2 %), while the  
315 variability of *A. tonsa* was mostly predicted by tintinnid abundance (27.0 %), salinity (18.7  
316 %), turbidity (12.2 %) and wind direction (11.7 %). Taken together, wind speed, wind  
317 direction and turbidity explained 62.2, 39.4 and 29.8 % of tintinnids, oligotrichs and *A.*  
318 *tonsa* variability, respectively. Partial dependence plots (Fig. 8) revealed that tintinnids and  
319 *A. tonsa* adults showed a saturating relationship with wind speed, with a threshold value  
320 near  $25 \text{ m s}^{-1}$ . Similarly, tintinnids and *A. tonsa* adults showed a binomial-like relationship  
321 with winds direction, i.e., the highest abundance values occurred in concurrence with winds  
322 coming from the SE quadrant and lowest abundance values in concurrence with winds  
323 coming from the NW quadrant. A dome-like pattern to water turbidity was register in all  
324 zooplankton groups, with the highest abundance values occurring at nearly 50 NTU.

325

326 **Discussion**

327 *Ciliates and A. tonsa interannual response*

328 During the studied period (1986–2009), we identified a progressive decline of tintinnids  
329 and *A. tonsa* adults and a less obvious decline on oligotrichs concentration. Parallel to the  
330 negative trend of zooplankton groups, phytoplankton community showed a drastic erosion  
331 of seasonal peaks and a shift from the typical unimodal productivity pattern to a bimodal  
332 regime (López-Abbate et al. 2017). Along the time series, two tintinnids species,  
333 *Tintinnopsis brasiliensis* and *T. sp.*, showed a positive trend. The oral diameter of these  
334 species ranges from 56 to 90  $\mu\text{m}$ , which is above the mean oral diameter of the estuarine  
335 tintinnids (mean  $<40 \mu\text{m}$ ). The oral area is proportional to prey encounter rate, and a wider  
336 encounter radius may confer a competitive advantage against species with narrower oral  
337 area constrained to a smaller prey size spectrum (Dolan 2010). The loss of the winter  
338 phytoplankton bloom in the last three decades, produced a loss of synchrony between  
339 tintinnids and primary producers, and changed the seasonal pattern of resource availability  
340 for higher trophic levels. In turn, the abundance of the dominant copepod *A. tonsa*, showed  
341 a significant positive relationship with tintinnids, denoting that the ecological interaction  
342 among groups was dominated by the bottom-up control exerted upon the copepod. In  
343 addition, the type of interaction confirmed by our model, allows to confidently attribute the  
344 negative trend of tintinnids to environmental factors. Tintinnids are a relevant prey item  
345 among estuarine copepod's diet (Dolan and Gallegos 2001), and during warm months in the  
346 Bahía Blanca Estuary, tintinnids represent nearly 78 % of total particles filtration by the  
347 copepod *A. tonsa* (Diodato and Hoffmeyer 2008). Our results revealed that environmental  
348 factors produced cascade-up effects, from phytoplankton to copepods, and imply a high  
349 probability that such effects resonate into the dynamics of planktivorous fish that prey on *A.*  
350 *tonsa* (López Cazorla et al. 2011). The disclosure of long-term patterns further highlights

351 the importance of sustained ocean observation systems to discriminate directional trends on  
352 ciliates and to identify clues regarding the loss of functional diversity.

353

354 *Long-term patterns of wind and water turbidity*

355 Regional wind patterns evidenced a shift toward low intensity but highly persistent NW  
356 winds in the last 25 years. Local winds over the South Atlantic are modulated by the  
357 intensity and displacement of the South Atlantic subtropical anticyclone (Venegas et al.  
358 1996, Palma et al. 2004). In the last decades, this anticyclone revealed a slight southward  
359 movement (Dragani et al. 2010) and caused wind pattern modifications over the region  
360 (Simionato et al. 2005, Brendel et al. 2017). At the interannual time scale, the southward  
361 displacement of the anticyclone tends to be associated with positive phases of SAM (Sun et  
362 al. 2017). Such large scale atmospheric variability was superimposed with the variability of  
363 local winds as suggested by our SEM model, in which both wind speed and wind direction  
364 showed teleconnections with SAM through the effect of sea level pressure anomalies. At  
365 longer timescales, the non-annular component of SAM produces contrasting spatial  
366 responses on SST and could also influence local wind patterns (Yeo and Kim 2015). In  
367 fact, a noticeable inflection in both wind speed and direction was perceived around 1999  
368 (Fig. 6a), in concurrence with the decadal shift on SAM spatial structure.

369 Although the increase of water turbidity is generally attributed to an increase in wind speed  
370 (Bever et al. 2018), in geomorphologically complex systems, other attributes such as the  
371 prevailing wind direction also come into play. The prominent role of wind direction on  
372 water turbidity revealed by the data, can be interpreted as the potential of winds cardinally  
373 aligned with the estuarine main channels to produce longer fetch and high energy wind  
374 waves (Perillo and Sequeira 1989, Pratolongo et al. 2010). High energy wind waves boost

375 the lateral erosion of wide expansions of tidal flats and promote the mobilization of soft  
376 sediments to the water column thereby contributing to increase water turbidity (Piccolo et  
377 al. 2008). Among estuaries with strong interaction across coastal forms (i.e. saltmarshes  
378 and flood-plains) and the water column, wind attributes capable of producing wind waves  
379 are thereby better descriptors of water turbidity than wind velocity alone (Cho 2007,  
380 Reisinger et al. 2017). The simultaneous intensification of bottom shear stress due to the  
381 expansion of the dredged area may additionally amplify the effect of changing wind  
382 patterns on water turbidity (López-Abbate et al. 2017).

383 The significant positive effect of SST on turbidity denotes the recurrent seasonal pattern of  
384 this variable, which typically shows maximum values during the warm months. This  
385 seasonal pattern is echoed by the dynamics of the borrowing crab, *Neohelice granulata*,  
386 which produces an intense sediment destabilization within tidal flats and a conspicuous  
387 mobilization of soft sediments toward the water column during summer (Zapperi et al.  
388 2016). The present rate of sea level transgression into the estuarine basin may also affect  
389 the positive trend of water turbidity (Lanfredi et al. 1988). Sea level rise presently causes an  
390 intense lateral erosion of saltmarshes which already experienced a 33 % loss of its area  
391 since 1967 (Pratolongo et al. 2013). Marsh boundary erosion along with the 50 % loss of  
392 shrub-like steep areas due to the settlement of human infrastructure (Pratolongo et al.  
393 2013), likely stimulated the continuous transport of mud deposits to the adjacent water  
394 column.

395

#### 396 *Partial response of zooplankton groups to wind patterns and water turbidity*

397 Long-term evaluation of environmental and biotic data revealed a prominent role of wind  
398 and water turbidity as underlying drivers of the decline of zooplankton groups, especially

399 tintinnids. In turn, the consistent increase on water turbidity resulted from the joint effect of  
400 wind patterns and the indirect effect of SAM in the last two decades. Further external forces  
401 may improve the consistency of predictive models constructed here. For instance,  
402 behavioural retention, migration and horizontal advection, are important factors that drive  
403 the spatial distribution of ciliates and their assessment requires a detailed three-dimensional  
404 observation of biota.

405 Partial dependence plots, denoted that wind speed produced a logistic-like pattern in the  
406 concentration of tintinnids and *A. tonsa*, while oligotrichs evidenced a dome-like pattern.  
407 Wind mixing is one of the most important drivers that determines three-dimensional  
408 distribution of plankton in shallow environments (Moreno-Ostos et al. 2008, Cardoso and  
409 Motta Marques 2009, Zhou et al. 2015). Additionally, wind-driven water turbulence may  
410 enhance or reduce prey encounter depending on the size of organisms, sensory strategies  
411 and behavioural traits (Pécseli et al. 2014). Ambush feeders such as *A. tonsa* when offered  
412 motile prey, are more dependent on turbulence to effectively encounter prey than  
413 motionless predators, while suspension feeders that create feeding currents, such as most  
414 ciliates, are less dependent on turbulence (Kiørboe and Saiz 1995). However, turbulence  
415 also affects ciliate's growth and sinking rate and their response is thereby less generalizable  
416 (Martínez et al. 2017). Fast-sinking tintinnids with agglomerated lorica, would be more  
417 dependent on wind-induced turbulence than slower sinking oligotrichs to retain suspended  
418 populations. The broad majority of the tintinnid species found in the estuary display  
419 agglutinated minerals, mostly sediments, covering the surface of their lorica, and this  
420 particular trait could underlie the specific response of both tintinnids and oligotrichs to  
421 wind speed.

422 Tintinnids and *A. tonsa* showed the strongest dependence on wind direction and evidenced  
423 a negative relationship with winds coming from the NW quadrant. In the Bahía Blanca  
424 Estuary, NW winds are effective impellers of erosive wind waves, and water turbidity can  
425 thereby be described as a function of wind direction (Piccolo et al. 2008). Accordingly, the  
426 response of plankton to wind direction is likely mediated by water turbidity, although wind  
427 direction may also affect the vertical distribution and retention of organisms. Wind-induced  
428 internal waves, for instance, reduce the likelihood of sedimentation losses (Hingsamer et al.  
429 2014). Waves generated by NW winds across the estuary have relatively small wavelengths  
430 implying that the turnover due to waves only occurs in the upper 2-3 m (Perillo and  
431 Sequeira 1989). The confinement of turbulence mixing within the upper layers likely  
432 intensifies the sedimentation of rapidly sinking plankton such as tintinnids. Our models,  
433 however, are based on the abundance of organisms at the surface layer, and do not provide  
434 evidence on the sedimentation of organisms or the compensatory dynamics such as vertical  
435 migration. NW winds are further directed toward the mouth of the estuary and can intensify  
436 the ebb-oriented transport of suspensoids toward the shelf area. Outflowing winds are  
437 known to produce the horizontal advection of plankton and the local exclusion of cells  
438 (Wolfe et al. 2015), and may be an additional factor driving the negative trend of tintinnids  
439 and *A. tonsa* to NW winds.

440 Water turbidity produced a dome-like pattern in zooplankton groups denoting that the  
441 highest abundance values occur under moderate levels of turbidity. Increased concentration  
442 of suspended sediments in the size range of zooplankton prey, limits prey encounter rate  
443 and handling (Boenigk and Novarino 2004). In fact, experimental data revealed that water  
444 turbidity reduced the growth and survival of heterotrophic nanoflagellates owing to the  
445 interference of mineral suspensoids with the uptake of prey rather than to the physical

446 damage of cells (Sommaruga and Kandolf 2014). In particular, the mean oral diameter of  
447 the 20 tintinnid species reported in the Bahía Blanca Estuary was 41  $\mu\text{m}$ , suggesting that  
448 the size spectrum of prey are below 10-15  $\mu\text{m}$  (Dolan et al. 2012). The prey size spectrum  
449 of tintinnids fall well between the size range of suspended sediments in the Bahía Blanca  
450 Estuary, which varies between 1-50  $\mu\text{m}$  while the modal value is 10  $\mu\text{m}$  (Guinder et al.  
451 2015). Above 50 NTU, water turbidity produced a negative effect on zooplankton groups,  
452 denoting that this factor may be considered as an ecological disturbance. Maximum  
453 zooplankton biomass, however, occurred at intermediate values of water turbidity,  
454 revealing that tintinnids, oligotrichs and *A. tonsa* are able to successfully coexist under this  
455 scenario. Optimal coexistence of functional groups at the average scale gradient of  
456 disturbance (i.e. water turbidity), partly supports the Intermediate Disturbance Hypothesis,  
457 which states that species diversity is maximized when disturbance intervals are  
458 intermediate (Connell 1978). Optimal disturbance interval depends on the generation time  
459 of the exposed organisms (Gaedeke and Sommer 1986), which in this case ranges between  
460 days to hours, and coincides with the time-lag needed to wind and tides to produce  
461 observable shifts in water turbidity (Perillo 1995).

462 At the long temporal scale, water turbidity may have produced a detrimental effect on  
463 ciliates by reducing the ratio between inedible suspensoids and phytoplankton, and forcing  
464 ciliates to an additional energy expenditure to sort inedible particles. Mixotrophic  
465 oligotrichs, however, are less sensitive to water turbidity and likely constitute the trophic  
466 link between bacteria and higher trophic levels due to the exclusion of light limited  
467 phytoplankton and filter feeders (Sommaruga and Kandolf 2014, Kammerlander et al.  
468 2016). The close link between oligotrichs and inorganic nutrients revealed by BRT denotes  
469 that higher inorganic nutrient concentration in the last years may have mitigated the low

470 concentration of prey availability. Wind-induced processes can thereby influence the food  
471 web organization by changing the spatial distribution of plankton and the ratio between  
472 edible and inedible particles.

473 Human activities at coastal areas are restricting the ability of coastal wetlands to  
474 compensate the effect of climate change, and projection based on the IPCC mean sea level  
475 rise scenario revealed that 20 % of salt-marsh area will be lost by 2100 (Craft et al. 2009).  
476 The cumulative effect of sea level rise along with intense land use and limited ecosystem  
477 feedbacks, will enhance the erosion of coastal margins and the mobilization of soft  
478 sediments toward the adjacent water column (Kirwan and Megonigal 2013). Shallow  
479 ecosystems with internal sources of suspended sediments, are thereby highly vulnerable to  
480 erosive processes. Our results provide quantitative evidence on the long-term response of  
481 pelagic ciliates to growing water turbidity and further revealed that ciliates can propagate  
482 such effects through the interannual variability of copepods.

483

#### 484 **Acknowledgment**

485 We thank Raúl Asteasuain and the staff from the IADO's Marine Chemistry Lab for the  
486 collection and analysis of samples. We are also grateful to Walter Melo for providing the  
487 study map. This study was supported by the National Agency for Promotion of Science and  
488 Technology (ANPCyT) (PIP D-738/2010) the National Scientific and Technical Research  
489 Council (CONICET) and by the Instituto Argentino de Oceanografía, (CONICET-UNS).

490

#### 491 **Figure and table captions**

492 **Figure 1.** Map of the Bahía Blanca Estuary, SW Atlantic Ocean, showing the location of  
493 the sampling site at the inner estuary close to "Puerto Cuatrerros". Main tributaries, sewer

494 discharge points, industrial and port areas (grey area) and the main urban centers (orange  
495 area) are also shown. Dredging operations take place periodically in the port area and in the  
496 Principal Channel.

497

498 **Figure 2.** Long-term changes of tintinnids, oligotrichs (cell  $l^{-1}$ , upper and mid panels,  
499 respectively) and *Acartia tonsa* (ind  $m^{-3}$ , lower panel) abundance. Significant trends are  
500 indicated by a linear fit and confidence interval at 95 %.  $R^2$  and p-values are indicated  
501 inside the plots.

502

503 **Figure 3.** Mean annual log-transformed abundance (cell  $l^{-1}$ ) of tintinnid species over the  
504 time series. Years with incomplete monthly observations (1986-1989, 1996-1997 and 2004-  
505 2006) were averaged together. Negative trend was observed in almost all species except for  
506 *Tintinnopsis brasiliensis* and *T. sp.* that showed a positive trend. Scale bar denotes the value  
507 of tintinnid abundance.

508

509 **Figure 4.** GAM estimates of mean monthly log-transformed abundance (cell  $l^{-1}$ ) of  
510 tintinnids in the periods 1986-2002 (blue dots) and 2003-2011 (red dots) denoting the loss  
511 of the spring peak following the winter phytoplankton bloom in recent years.  $R^2$  and p-  
512 values are indicated inside the plots.

513

514 **Figure 5.** Annual wind roses in the period 1991-2015 showing the frequency of wind speed  
515 and direction (%). Plots denotes the decreased prevalence of wind coming from the NE, SE  
516 and SW quadrants. Mean wind velocity decreased after 2000 and the relative persistence of

517 NW winds intensified over the time series. Scale bar at the right side of the plots denotes  
518 wind speed (ws).

519

520 **Figure 6.** a) Annual mean of wind speed (upper panel), wind direction (mid panel) and  
521 turbidity (lower panel) in the Bahía Blanca Estuary over the period 1978–2011. b) Path  
522 diagrams showing significant ( $p < 0.05$ ) interconnections between climate and  
523 environmental drivers and water turbidity. At each significant path the positive (blue) and  
524 negative (red) effects are represented by the standardized coefficients. The variables used in  
525 SEM were: SAM-Marshall index (SAM), Niño 3.4 index (N3.4), sea level pressure (SLP),  
526 air temperature (Air Temp), precipitation (PP), wind speed (ws), wind direction (wd), sea  
527 surface temperature (SST) and turbidity (turb).

528

529 **Figure 7.** The ranking of explanatory variable importance driving the response of tintinnids  
530 (left panel) and oligotrichs (right panel) abundance. The variables used in the BRT model  
531 were wind speed (ws), wind direction (wd), turbidity (turb), chlorophyll concentration  
532 (chl<sub>a</sub>), salinity (sal), dissolved inorganic nitrogen (DIN), phosphate (P) and silicate (Si).  $R^2$   
533 values are indicated inside the plots.

534

535 **Figure 8.** Partial dependence plots for wind speed (ws), wind direction (wd) and turbidity  
536 as depicted by BRT of zooplankton groups: a) tintinnids, b) oligotrichs and c) *Acartia*  
537 *tonsa*. Percentage of explained variance of each predictor is shown between parentheses.

538

539 **References**

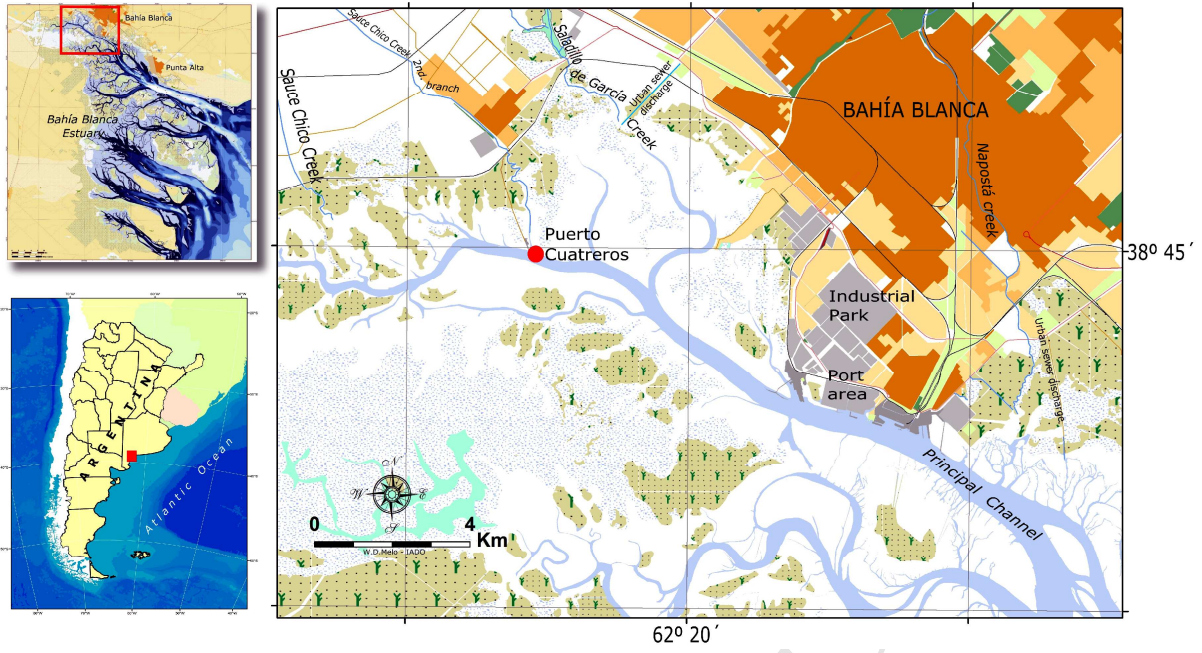
- 540 Aberle, N., K. G. Schulz, A. Stühr, A. M. Malzahn, A. Ludwig, and U. Riebesell. 2013.  
541 High tolerance of microzooplankton to ocean acidification in an Arctic coastal  
542 plankton community. *Biogeosciences* **10**:1471-1481.
- 543 Alsterberg, C., J. S. Eklöf, L. Gamfeldt, J. N. Havenhand, and K. Sundbäck. 2013.  
544 Consumers mediate the effects of experimental ocean acidification and warming on  
545 primary producers. *Proceedings of the National Academy of Sciences*:201303797.
- 546 Aravena, J. C. and B. H. Luckman. 2009. Spatio-temporal rainfall patterns in Southern  
547 South America. *International Journal of Climatology* **29**:2106-2120.
- 548 Barría de Cao, M. S., D. Beigt, and C. Piccolo. 2005. Temporal variability of diversity and  
549 biomass of tintinnids (Ciliophora) in a southwestern Atlantic temperate estuary.  
550 *Journal of Plankton Research* **27**:1103-1111.
- 551 Barton, A. D., B. A. Ward, R. G. Williams, and M. J. Follows. 2014. The impact of fine-  
552 scale turbulence on phytoplankton community structure. *Limnology and*  
553 *Oceanography: Fluids and Environments* **4**:34-49.
- 554 Bever, A. J., M. L. MacWilliams, and D. K. Fullerton. 2018. Influence of an observed  
555 decadal decline in wind speed on turbidity in the San Francisco Estuary. *Estuaries*  
556 *and Coasts*.
- 557 Boenigk, J. and G. Novarino. 2004. Effect of suspended clay on the feeding and growth of  
558 bacterivorous flagellates and ciliates. *Aquatic Microbial Ecology* **34**:181-192.
- 559 Boltovskoy, D. 1981. Atlas del zooplancton del Atlántico Sudoccidental y métodos de  
560 trabajo con el zooplancton marino. Instituto Nacional de Investigación y Desarrollo  
561 Pesquero Mar del Plata.
- 562 Boyd, P. W. and D. A. Hutchins. 2012. Understanding the responses of ocean biota to a  
563 complex matrix of cumulative anthropogenic change. *Marine Ecology Progress*  
564 *Series* **470**:125-135.
- 565 Brand, A., J. R. Lacy, K. Hsu, D. Hoover, S. Gladding, and M. T. Stacey. 2010. Wind-  
566 enhanced resuspension in the shallow waters of South San Francisco Bay:  
567 Mechanisms and potential implications for cohesive sediment transport. *Journal of*  
568 *Geophysical Research: Oceans* **115**.
- 569 Breiman, L., J. Friedman, C. Stone, and R. Olshen. 1984. *Classification and Regression*  
570 *Trees*. CRC Press, New York.
- 571 Brendel, A. S., M. S. Duttó, M. C. Menéndez, M. A. H. Cisneros, and M. C. Piccolo. 2017.  
572 Wind Pattern Change Along a Period of Coastal Occurrence Variation of a Stinging  
573 Medusa on a SW Atlantic Beach. *Anuário do Instituto de Geociências - UFRJ*  
574 **40**:303-315.
- 575 Calbet, A. and E. Saiz. 2005. The ciliate-copepod link in marine ecosystems. *Aquatic*  
576 *Microbial Ecology* **38**:157-167.
- 577 Cardoso, L. d. S. and D. d. Motta Marques. 2009. Hydrodynamics-driven plankton  
578 community in a shallow lake. *Aquatic Ecology* **43**:73-84.
- 579 Clamp, J. C. and D. H. Lynn. 2017. Investigating the biodiversity of ciliates in the 'Age of  
580 Integration'. *Eur J Protistol* **61**:314-322.
- 581 Connell, J. H. 1978. Diversity in tropical rain forests and coral reefs. *Science* **199**:1302-  
582 1310.
- 583 Craft, C., J. Clough, J. Ehman, S. Joye, R. Park, S. Pennings, H. Guo, and M. Machmuller.  
584 2009. Forecasting the effects of accelerated sea-level rise on tidal marsh ecosystem  
585 services. *Frontiers in Ecology and the Environment* **7**:73-78.

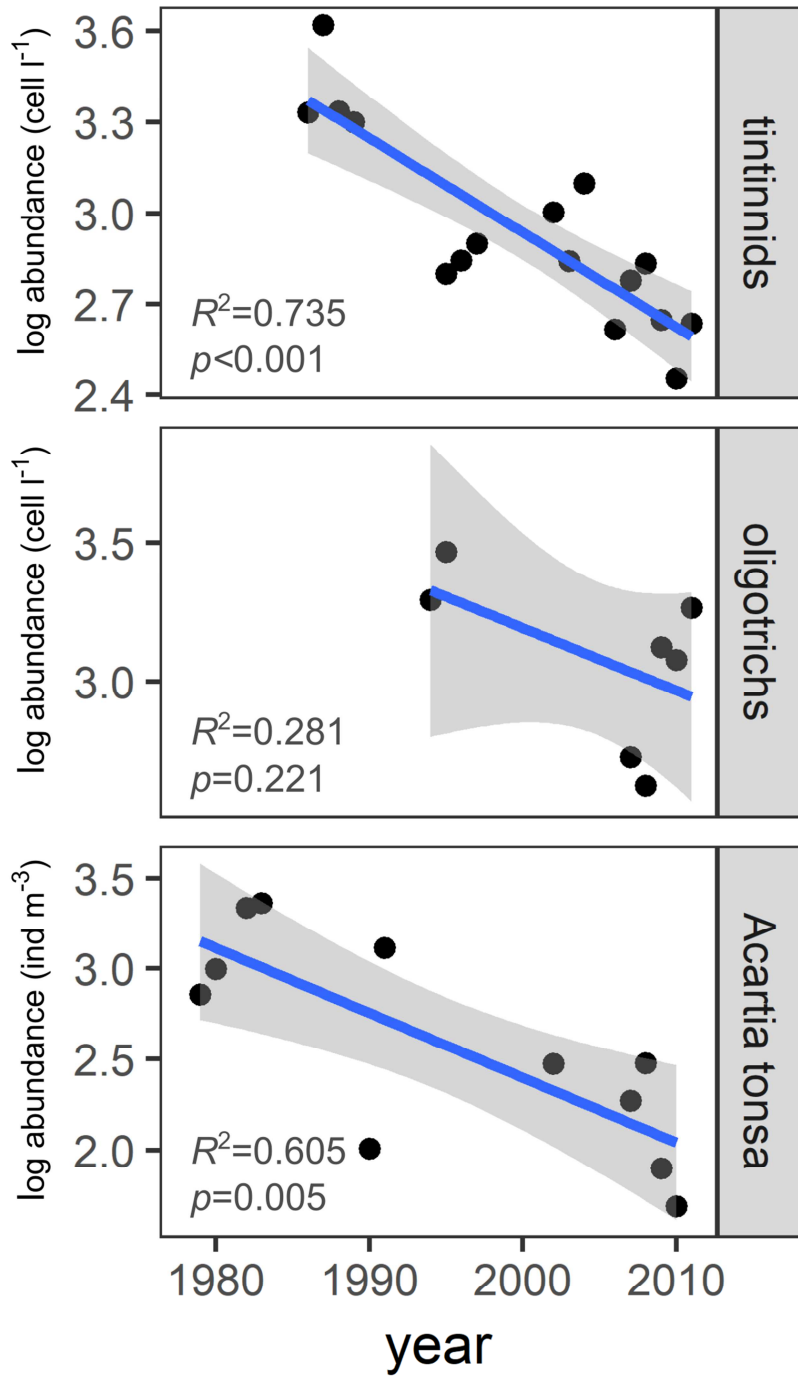
- 586 Cho, H. J. 2007. Effects of prevailing winds on turbidity of a shallow estuary. *International*  
587 *Journal of Environmental Research and Public Health* **4**:185-192.
- 588 De'ath, G. and K. E. Fabricius. 2000. Classification and regression trees: a powerful yet  
589 simple technique for ecological data analysis. *Ecology* **81**:3178–3192.
- 590 Diodato, S. L. and M. S. Hoffmeyer. 2008. Contribution of planktonic and detritic fractions  
591 to the natural diet of mesozooplankton in Bahía Blanca Estuary. *Hydrobiologia*  
592 **614**:83-90.
- 593 Dolan, J. R. 2010. Morphology and ecology in tintinnid ciliates of the marine plankton:  
594 correlates of lorica dimensions. *Acta Protozoologica* **2010**:235-244.
- 595 Dolan, J. R. and C. L. Gallegos. 2001. Estuarine diversity of tintinnids (planktonic ciliates).  
596 *Journal of Plankton Research* **23**:1009-1027.
- 597 Dolan, J. R., R. W. Pierce, E. J. Yang, and S. Y. Kim. 2012. Southern ocean biogeography  
598 of tintinnid ciliates of the marine plankton. *J Eukaryot Microbiol* **59**:511-519.
- 599 Dragani, W. C., P. B. Martin, C. G. Simionato, and M. I. Campos. 2010. Are wind wave  
600 heights increasing in south-eastern south American continental shelf between 32°S  
601 and 40°S? *Continental Shelf Research* **30**:481-490.
- 602 Elith, J., J. R. Leathwick, and T. Hastie. 2008. A working guide to boosted regression trees.  
603 *Journal of Animal Ecology* **77**:802-813.
- 604 Fogt, R. L., D. H. Bromwich, and K. M. Hines. 2011. Understanding the SAM influence on  
605 the South Pacific ENSO teleconnection. *Climate Dynamics* **36**:1555-1576.
- 606 Gaedeke, A. and U. Sommer. 1986. The influence of the frequency of periodic disturbances  
607 on the maintenance of phytoplankton diversity. *Oecologia* **71**:25-28.
- 608 Guinder, V. A., M. C. López-Abbate, A. A. Berasategui, V. L. Negrin, G. Zapperi, P. D.  
609 Pratolongo, M. D. Fernández Severini, and C. A. Popovich. 2015. Influence of the  
610 winter phytoplankton bloom on the settled material in a temperate shallow estuary.  
611 *Oceanologia* **57**:50-60.
- 612 Guinder, V. A., C. A. Popovich, J. C. Molinero, and G. M. Perillo. 2010. Long-term  
613 changes in phytoplankton phenology and community structure in the Bahía Blanca  
614 Estuary, Argentina. *Marine Biology* **157**:2703-2716.
- 615 Hasle, G. R. 1978. The inverted microscope method. Pages 88-96 in A. Sournia, editor.  
616 *Phytoplankton Manual*. UNESCO, Paris.
- 617 Heger, T. J., V. P. Edgcomb, E. Kim, J. Lukes, B. S. Leander, and N. Yubuki. 2014. A  
618 resurgence in field research is essential to better understand the diversity, ecology,  
619 and evolution of microbial eukaryotes. *J Eukaryot Microbiol* **61**:214-223.
- 620 Hingsamer, P., F. Peeters, and H. Hofmann. 2014. The consequences of internal waves for  
621 phytoplankton focusing on the distribution and production of *Planktothrix*  
622 *rubescens*. *PLoS One* **9**:e104359.
- 623 Jack, J. D. and J. J. Gilbert. 1993. The effect of suspended clay on ciliate population growth  
624 rates. *Freshw Biol* **29**:385-394.
- 625 Kammerlander, B., K. A. Koinig, E. Rott, R. Sommaruga, B. Tartarotti, F. Trattner, and B.  
626 Sonntag. 2016. Ciliate community structure and interactions within the planktonic  
627 food web in two alpine lakes of contrasting transparency. *Freshw Biol* **61**:1950-  
628 1965.
- 629 Keller, D. P. and R. R. Hood. 2011. Modeling the seasonal autochthonous sources of  
630 dissolved organic carbon and nitrogen in the upper Chesapeake Bay. *Ecological*  
631 *modelling* **222**:1139-1162.
- 632 Kiørboe, T. 2008. A mechanistic approach to plankton ecology. Princeton University Press.

- 633 Kjørboe, T. and E. Saiz. 1995. Planktivorous feeding in calm and turbulent environments,  
634 with emphasis on copepods. *Marine Ecology Progress Series* **122**:135-145.
- 635 Kirwan, M. L. and J. P. Megonigal. 2013. Tidal wetland stability in the face of human  
636 impacts and sea-level rise. *Nature* **504**:53.
- 637 Kreyling, J., A. H. Schweiger, M. Bahn, P. Ineson, M. Migliavacca, T. Morel-Journel, J. R.  
638 Christiansen, N. Schtickzelle, and K. S. Larsen. 2018. To replicate, or not to  
639 replicate – that is the question: how to tackle nonlinear responses in ecological  
640 experiments. *Ecol Lett* **0**.
- 641 Lanfredi, N. W., E. E. D'Onofrio, and C. A. Mazio. 1988. Variations of the mean sea level  
642 in the southwest Atlantic Ocean. *Continental Shelf Research* **8**:1211-1220.
- 643 Laspoumaderes, C., M. S. Souza, B. Modenutti, and E. Balseiro. 2017. Glacier melting and  
644 response of *Daphnia* oxidative stress. *Journal of Plankton Research* **39**:675-686.
- 645 Legendre, L. and R. B. Rivkin. 2015. Flows of biogenic carbon within marine pelagic food  
646 webs: Roles of microbial competition switches. *Marine Ecology Progress Series*  
647 **521**:19-30.
- 648 Li, Y. and M. Li. 2011. Effects of winds on stratification and circulation in a partially  
649 mixed estuary. *Journal of Geophysical Research: Oceans* **116**.
- 650 López-Abbate, M. C., J. C. Molinero, V. A. Guinder, M. S. Dutto, M. S. Barria de Cao, L.  
651 A. Ruiz Etcheverry, R. E. Pettigrosso, M. C. Carcedo, and M. S. Hoffmeyer. 2015.  
652 Microplankton dynamics under heavy anthropogenic pressure. The case of the  
653 Bahía Blanca Estuary, southwestern Atlantic Ocean. *Mar Pollut Bull* **95**:305-314.
- 654 López-Abbate, M. C., J. C. Molinero, V. A. Guinder, G. M. E. Perillo, R. H. Freije, U.  
655 Sommer, C. V. Spetter, and J. E. Marcovecchio. 2017. Time-varying environmental  
656 control of phytoplankton in a changing estuarine system. *Science of The Total*  
657 *Environment* **609**:1390-1400.
- 658 López Cazorla, A., R. Pettigrosso, L. Tejera, and R. Camina. 2011. Diet and food selection  
659 by *Ramnogaster arcuata* (Osteichthyes, Clupeidae). *Journal of fish biology* **78**:2052-  
660 2066.
- 661 Lorenzen, C. J. 1967. Determination of chlorophyll and pheo-pigments:  
662 Spectrophotometric equations. *Limnology and Oceanography* **12**:343-346.
- 663 Marshall, G. J. 2003. Trends in the Southern Annular Mode from observations and  
664 reanalyses. *Journal of Climate* **16**:4134-4143.
- 665 Martínez, R. A., A. Calbet, and E. Saiz. 2017. Effects of small-scale turbulence on growth  
666 and grazing of marine microzooplankton. *Aquatic Sciences* **80**:2.
- 667 Menéndez, C. G. and A. F. Carril. 2010. Potential changes in extremes and links with the  
668 Southern Annular Mode as simulated by a multi-model ensemble. *Climatic change*  
669 **98**:359-377.
- 670 Mitra, A., K. J. Flynn, J. M. Burkholder, T. Berge, A. Calbet, J. A. Raven, E. Granéli, P. M.  
671 Glibert, P. J. Hansen, D. K. Stoecker, F. Thingstad, U. Tillmann, S. Våge, S.  
672 Wilken, and M. V. Zubkov. 2014. The role of mixotrophic protists in the biological  
673 carbon pump. *Biogeosciences* **11**:995-1005.
- 674 Moreno-Ostos, E., L. Cruz-Pizarro, A. Basanta, and D. G. George. 2008. The influence of  
675 wind-induced mixing on the vertical distribution of buoyant and sinking  
676 phytoplankton species. *Aquatic Ecology* **43**:271-284.
- 677 Palma, E. D., R. P. Matano, A. R. Piola, and L. E. Sitz. 2004. A comparison of the  
678 circulation patterns over the Southwestern Atlantic Shelf driven by different wind  
679 stress climatologies. *Geophysical Research Letters* **31**.

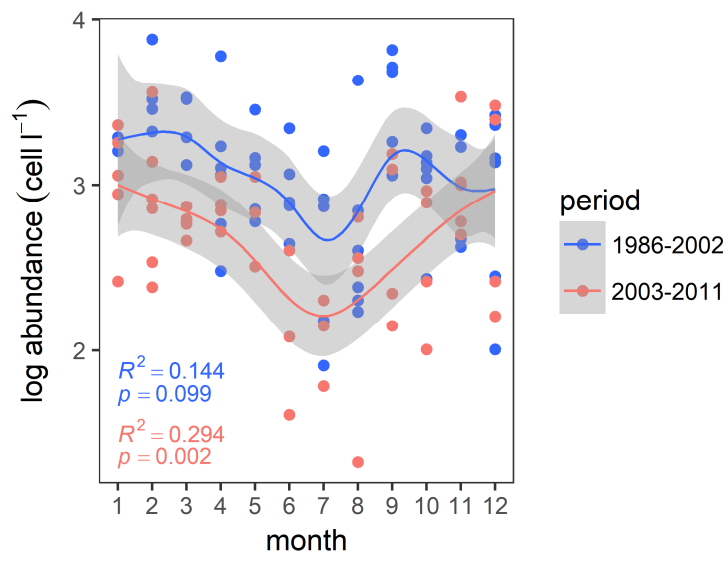
- 680 Pécseli, H., J. Trulsen, and Ø. Fiksen. 2014. Predator–prey encounter and capture rates in  
681 turbulent environments. *Limnology and Oceanography: Fluids and Environments*  
682 **4**:85-105.
- 683 Perillo, G. M. 1995. *Geomorphology and sedimentology of estuaries*. Elsevier.
- 684 Perillo, G. M. E. 2009. Tidal courses: classification, origin and functionality. Pages 185–  
685 210 in G. M. E. Perillo, E. Wolanski, D. R. Cahoon, and M. M. Brinson, editors.  
686 *Coastal Wetlands: An Integrated Ecosystem Approach*. Elsevier, Amsterdam.
- 687 Perillo, G. M. E., M. C. Piccolo, E. Parodi, and R. H. Freije. 2001. The Bahía Blanca  
688 Estuary, Argentina. Pages 205-217 in U. Seeliger and B. Kjerfve, editors. *Coastal*  
689 *Marine Ecosystems of Latin America*. Springer Berlin Heidelberg, Berlin,  
690 Heidelberg.
- 691 Perillo, G. M. E. and M. E. Sequeira. 1989. Geomorphologic and sediment transport  
692 characteristics of the middle reach of the Bahía Blanca estuary (Argentina). *Journal*  
693 *of Geophysical Research: Oceans* **94**:14351-14362.
- 694 Pettigrosso, R. E. 2003. Planktonic ciliates Choreotrichida and Strombidiida from the inner  
695 zone of Bahía Blanca Estuary, Argentina. *Iheringia, Série Zoolgia* **93**:117-126.
- 696 Piccolo, M., G. Perillo, and W. Melo. 2008. The Bahía Blanca Estuary: an integrated  
697 overview of its geomorphology and dynamics. Pages 221-232. IST Scientific  
698 Publishers, Lisbon (Portugal).
- 699 Piccolo, M. C. and G. M. E. Perillo. 1990. Physical characteristics of the Bahía Blanca  
700 estuary (Argentina). *Estuarine, Coastal and Shelf Science* **31**:303-317.
- 701 Pratolongo, P., C. Mazzon, G. Zapperi, M. J. Piovan, and M. M. Brinson. 2013. Land cover  
702 changes in tidal salt marshes of the Bahía Blanca estuary (Argentina) during the  
703 past 40 years. *Estuarine, Coastal and Shelf Science* **133**:23-31.
- 704 Pratolongo, P., M. J. Piovan, D. G. Cuadrado, and E. A. Gómez. 2017. Coastal landscape  
705 evolution on the western margin of the Bahía Blanca Estuary (Argentina) mirrors a  
706 non-uniform sea-level fall after the mid-Holocene highstand. *Geo-Marine Letters*  
707 **37**:373-384.
- 708 Pratolongo, P. D., G. M. E. Perillo, and M. C. Piccolo. 2010. Combined effects of waves  
709 and plants on a mud deposition event at a mudflat-saltmarsh edge in the Bahía  
710 Blanca estuary. *Estuarine, Coastal and Shelf Science* **87**:207-212.
- 711 R Development Core Team. 2014. R: A language and environment for statistical  
712 computing.
- 713 Reisinger, A., J. C. Gibeaut, and P. E. Tissot. 2017. Estuarine suspended sediment  
714 dynamics: Observations derived from over a decade of satellite data. *Frontiers in*  
715 *Marine Science* **4**.
- 716 Reynolds, C. S. 2006. *The ecology of phytoplankton*. Cambridge University Press.
- 717 Scully, M. E., C. Friedrichs, and J. Brubaker. 2005. Control of estuarine stratification and  
718 mixing by wind-induced straining of the estuarine density field. *Estuaries* **28**:321-  
719 326.
- 720 Simionato, C. G., C. S. Vera, and F. Siegismund. 2005. Surface wind variability on  
721 seasonal and interannual scales over Río de la Plata area. *Journal of Coastal*  
722 *Research* **21**:770-783.
- 723 Sommaruga, R. and G. Kandolf. 2014. Negative consequences of glacial turbidity for the  
724 survival of freshwater planktonic heterotrophic flagellates. *Sci Rep* **4**:4113.
- 725 Spetter, C. V., C. A. Popovich, A. Arias, R. O. Asteasuain, R. H. Freije, and J. E.  
726 Marcovecchio. 2015. Role of nutrients in phytoplankton development during a

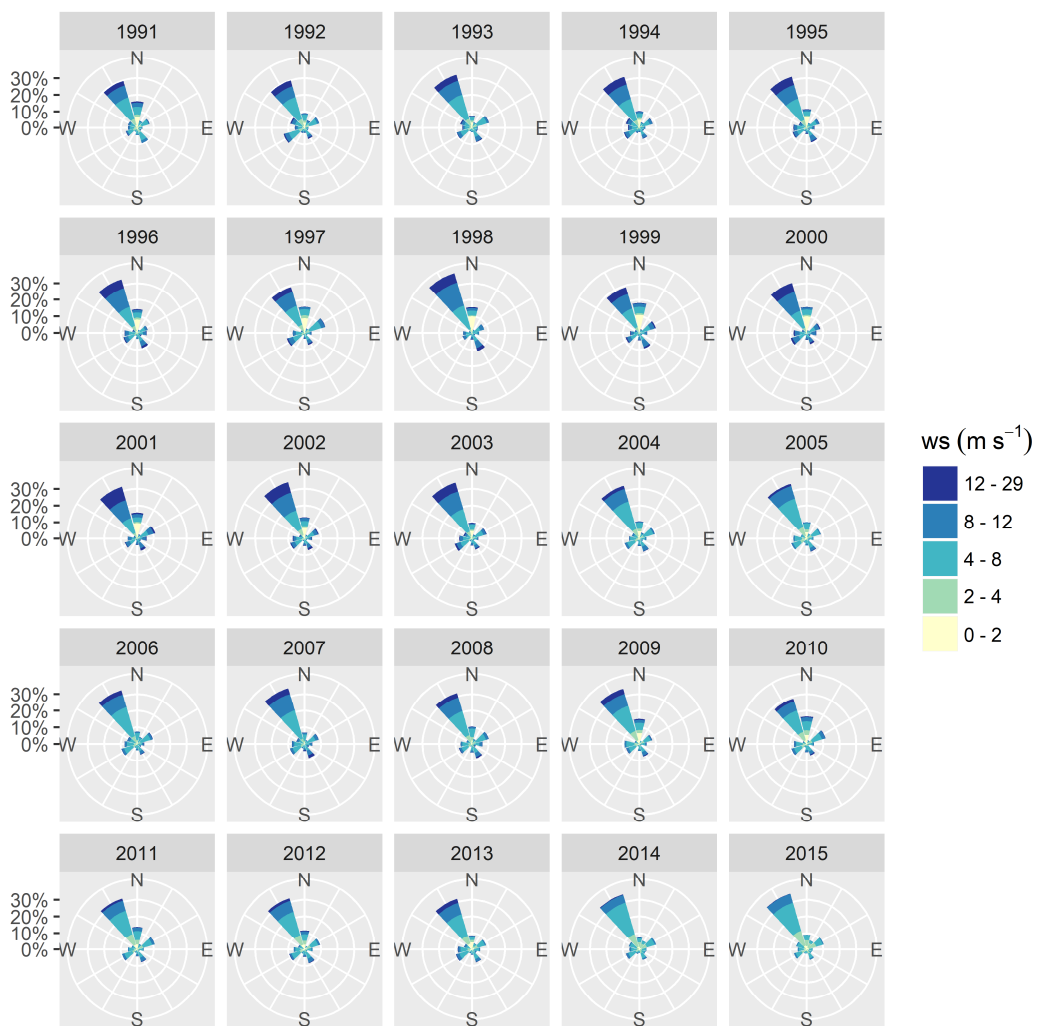
- 727 winter diatom bloom in a eutrophic South American estuary (Bahía Blanca,  
728 Argentina). *Journal of Coastal Research* **31**:76-87.
- 729 Steinberg, D. K. and M. R. Landry. 2017. Zooplankton and the ocean carbon cycle. *Ann*  
730 *Rev Mar Sci* **9**:413-444.
- 731 Sun, X., K. H. Cook, and E. K. Vizy. 2017. The South Atlantic Subtropical High:  
732 Climatology and Interannual Variability. *Journal of Climate* **30**:3279-3296.
- 733 Trenberth, K. E. 1997. The definition of el nino. *Bulletin of the American Meteorological*  
734 *Society* **78**:2771-2778.
- 735 Venegas, S. A., L. A. Mysakand, and D. N. Straub. 1996. Evidence for interannual and  
736 interdecadal climate variability in the South Atlantic. *Geophysical Research Letters*  
737 **23**:2673-2676.
- 738 Vera, C., G. Silvestri, V. Barros, and A. Carril. 2004. Differences in el nino response over  
739 the southern hemisphere. *Journal of Climate* **17**:1741-1753.
- 740 Weir, D. and J. McManus. 1987. The role of wind in generating turbidity maxima in the  
741 Tay estuary. *Continental Shelf Research* **7**:1315-1318.
- 742 Whipple, A. C., R. A. Luettich, J. V. Reynolds-Fleming, and R. H. Neve. 2018. Spatial  
743 differences in wind-driven sediment resuspension in a shallow, coastal estuary.  
744 *Estuarine, Coastal and Shelf Science* **213**:49-60.
- 745 Wohlers, J., A. Engel, E. Zollner, P. Breithaupt, K. Jurgens, H. G. Hoppe, U. Sommer, and  
746 U. Riebesell. 2009. Changes in biogenic carbon flow in response to sea surface  
747 warming. *Proc Natl Acad Sci U S A* **106**:7067-7072.
- 748 Wolfe, A. M., S. E. Allen, M. Hodal, R. Pawlowicz, B. P. Hunt, and D. Tommasi. 2015.  
749 Impact of advection loss due to wind and estuarine circulation on the timing of the  
750 spring phytoplankton bloom in a fjord. *ICES Journal of Marine Science* **73**:1589-  
751 1609.
- 752 Yeo, S.-R. and K.-Y. Kim. 2015. Decadal changes in the Southern Hemisphere sea surface  
753 temperature in association with El Niño–Southern Oscillation and Southern Annular  
754 Mode. *Climate Dynamics* **45**:3227-3242.
- 755 Zapperi, G., M. J. Piovan, and P. Pratolongo. 2017. Community structure and spatial  
756 zonation of benthic macrofauna in mudflats of the Bahía Blanca Estuary, Argentina.  
757 *Journal of Coastal Research* **0**:null.
- 758 Zapperi, G., P. Pratolongo, M. J. Piovan, and J. E. Marcovecchio. 2016. Benthic-Pelagic  
759 coupling in an intertidal mudflat in the Bahía Blanca Estuary (SW Atlantic). *Journal*  
760 *of Coastal Research* **32**:629-637.
- 761 Zhou, J., B. Qin, C. Casenave, X. Han, G. Yang, T. Wu, P. Wu, and J. Ma. 2015. Effects of  
762 wind wave turbulence on the phytoplankton community composition in large,  
763 shallow Lake Taihu. *Environmental Science and Pollution Research* **22**:12737-  
764 12746.

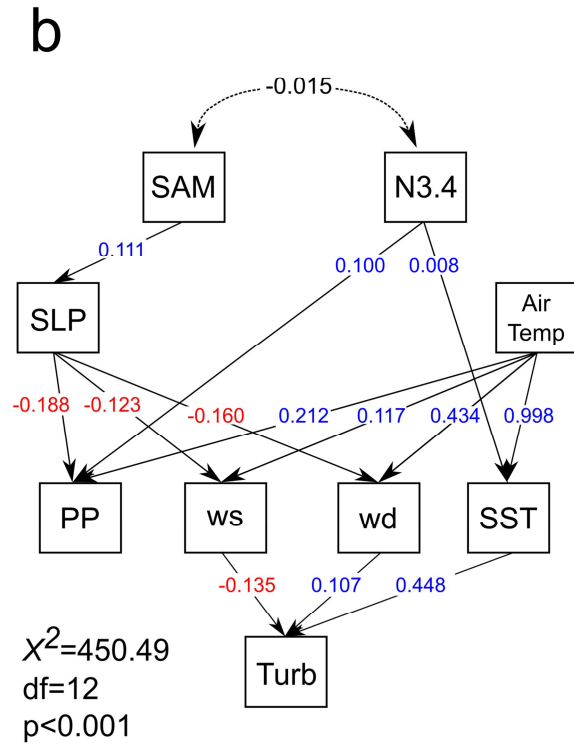
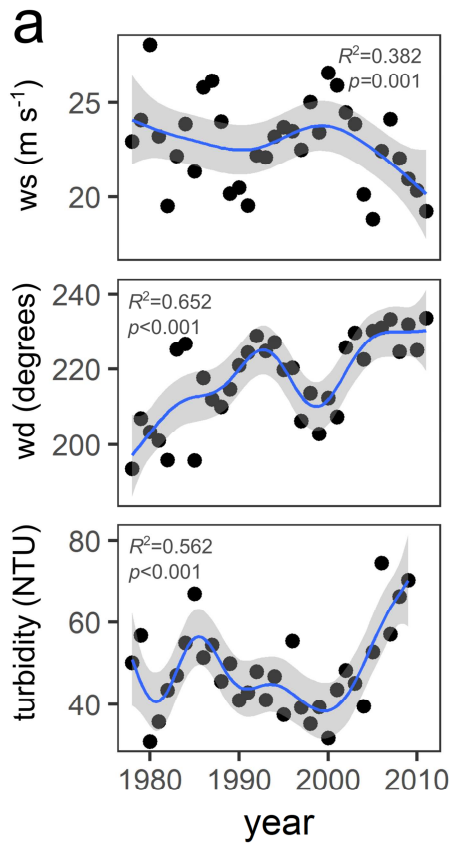


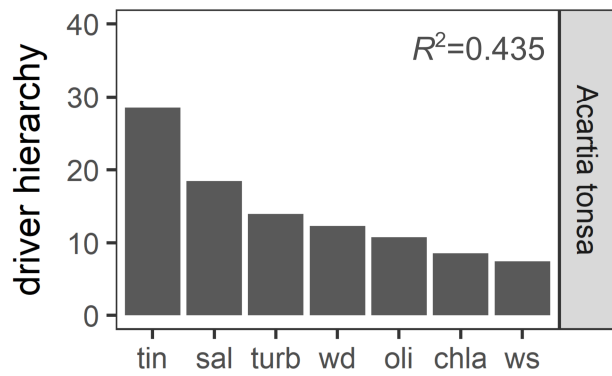
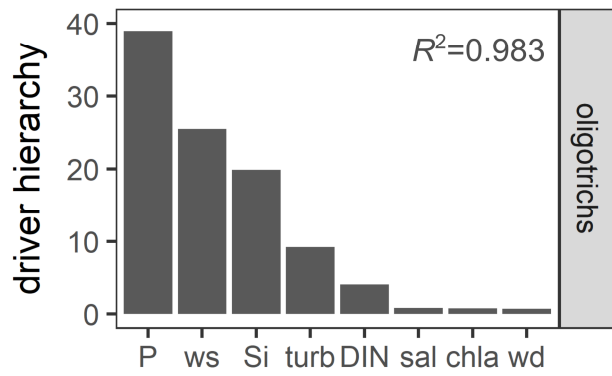
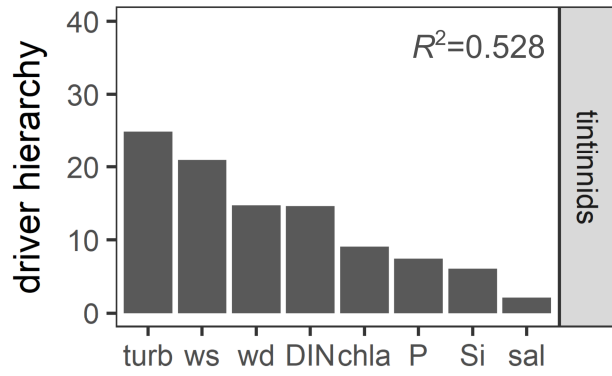


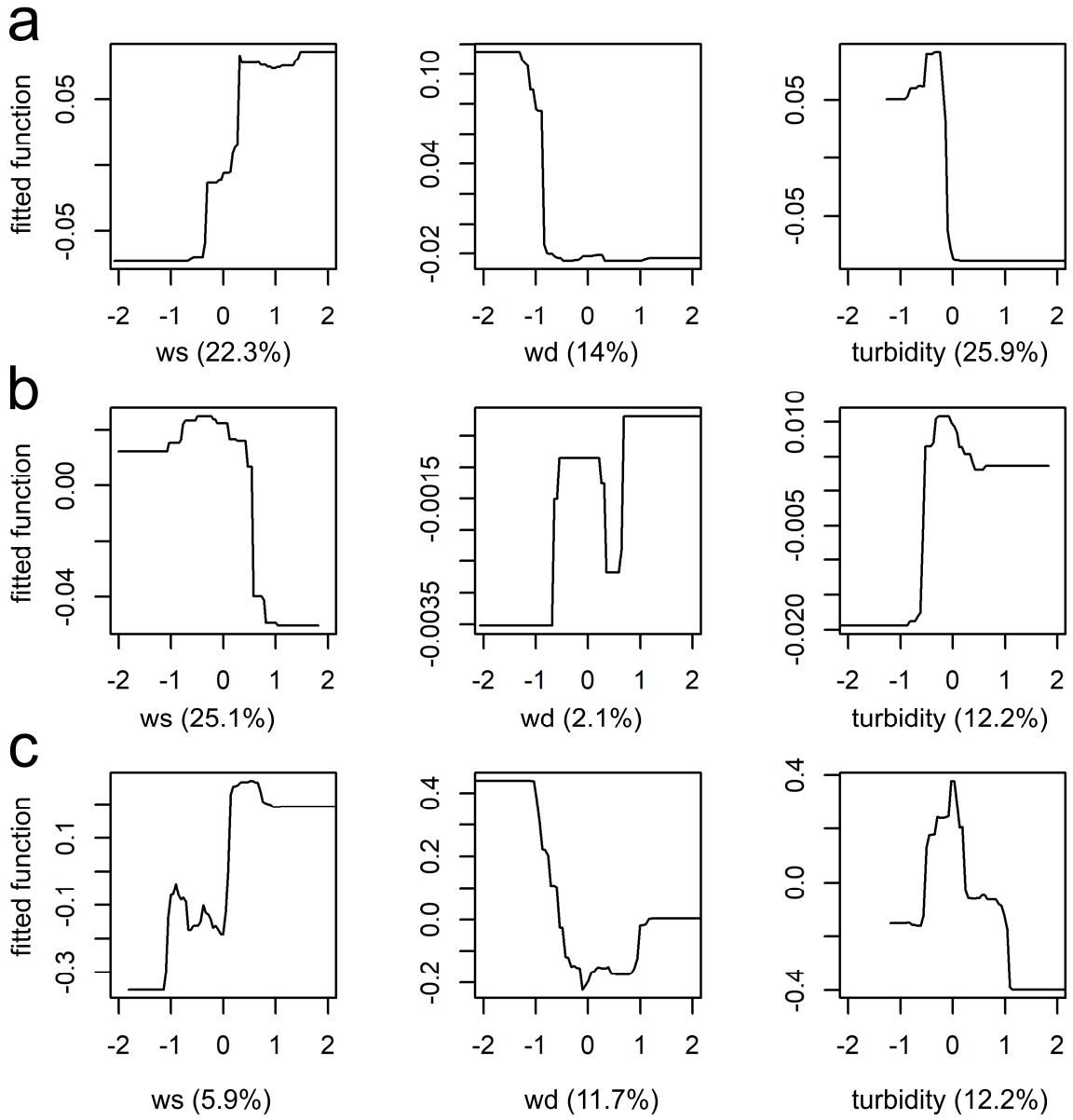












- Planktonic ciliate's abundance decreased over the last 25 years in a shallow estuary.
- Decreasing cell abundance was linked to changes in wind dominant regimes and increased water turbidity.
- Tintinnids were more vulnerable to wind patterns and turbidity and lost synchrony with primary productivity.
- Interannual variability of the copepod *Acartia tonsa* followed the changes in ciliate community.
- Erosive processes in shallow estuaries impact on the interannual dynamics of ciliates and such effects can cascade-up to copepods.